Published in final edited form as:
Mol Imaging. 2011 June ; 10(3): 168–7.

Microfluidic-based ^{18}F-labeling of Biomolecules for ImmunoPET

Kan Liu[1,2,3,4,7], **Eric J. Lepin**[2,3,4,7], **Ming-Wei Wang**[2,3,4,5], **Feng Guo**[2,3,4,6], **Wei-Yu Lin**[2,3,4], **Yi-Chun Chen**[2,3,4], **Shannon J. Sirk**[2,3,4], **Sebastian Olma**[2,3], **Michael E. Phelps**[2,3,4], **Xing-Zhong Zhao**[6], **Hsian-Rong Tseng**[2,3,4], **R. Michael van Dam**[2,3,4,8], **Anna M. Wu**[2,3,4,8], and **Clifton K.-F. Shen**[2,3,4,8]

[1]College of Electronics and Information Engineering, Wuhan Textile University, Wuhan, 430000, China

[2]Department of Molecular and Medical Pharmacology, David Geffen School of Medicine at University of California, Los Angeles, 23–120 Center for Health Science, Los Angeles, California 90095, USA

[3]Crump Institute for Molecular Imaging, 570 Westwood Plaza, Los Angeles, California 90095, USA

[4]California Nanosystems Institute, 570 Westwood Plaza, Los Angeles, California 90095, USA

[5]PET Center and Department of Nuclear Medicine, Cancer Hospital, Fudan University, Shanghai, 200032, China

[6]Department of Physics, School of Physics, and Center of Nanoscience and Nanotechnology, Wuhan University, Wuhan 430072, China

Abstract

Methods for tagging biomolecules with F-18 as immuno-Positron Emission Tomography (immunoPET) tracers require tedious optimization of radiolabeling conditions, and can consume large amounts of scarce biomolecules. We describe an improved method utilizing a digital microfluidic droplet generation (DMDG) chip which provides computer controlled metering and mixing of ^{18}F-tag, biomolecule, and buffer in defined ratios, allowing rapid scouting of reaction conditions in nanoliter volumes. The identified optimized conditions were then translated to bench-scale ^{18}F-labeling of a cancer-specific engineered antibody fragments, enabling microPET imaging of tumors in xenografted mice at 0.5–4 h post injection.

Keywords

ImmunoPET; microfluidics; droplet; [^{18}F]SFB; PSCA; antibody fragments; diabody

Introduction

Positron emission tomography (PET) is a molecular imaging technique for biomedical research, drug development and several clinical applications, including disease diagnosis/stage and assessment of therapeutic efficacy.[1, 2] In combination with specific radiotracers, PET provides noninvasive whole-body visualization and quantification of normal biochemical processes as well as the onset, extent and kinetics of pathological processes in

[8]Correspondence and reprint requests should be addressed to C.K.-F.S. (kshen@mednet.ucla.edu), A.M.W. (awu@mednet.ucla.edu) and R.M.V. (mvandam@mednet.ucla.edu).
[7]These authors contributed equally to this work.

diseases.[3] Immuno-Positron Emission Tomography (immuno-PET) capitalizes on the selectivity of antibodies and their fragments, and is emerging as an important approach for cancer imaging.[1] Recent advances in protein engineering have led to the generation of small antibody fragments and other protein binding scaffolds with high specificity and affinity to their targets; *in vivo*, these show good tumor targeting and accelerated blood clearance necessary for imaging. In clinical applications, fluorine-18 (F-18) offers advantages of short half-life ($T_{1/2}$=109.7 min), high positron yield (96.7%), and broad availability from existing radiopharmacy networks. With reduced molecular weights below the threshold for first-pass renal clearance, these proteins, when labeled with short-lived positron-emitters such as F-18, allow high-contrast, same-day imaging [1–6 h post injection (p.i.)]. Therefore, the combination of a rapid-targeting protein format with easily accessible F-18 has strong potential for clinical development.

Current methods for *direct* ^{18}F-labeling of small molecules using no-carried-added (n.c.a.) [^{18}F]fluoride often require anhydrous, strongly basic conditions at high temperature, which are not compatible with fragile biomolecules, such as proteins. Instead, the incorporation of [^{18}F]fluoride into proteins is usually achieved by using ^{18}F-labeled prosthetic groups, for example, N-succinimidyl 4-[^{18}F]fluorobenzoate ([^{18}F]SFB).[4] This is the most widely used ^{18}F-acylation reagent due to its *in vivo* stability and radiochemical yield.[5] However, recent studies on ^{18}F-labeling of antibody fragments using [^{18}F]SFB reported a low radiolabeling yield which has prevented their more widespread adoption for preclinical studies and clinical translation.[6]

It is well established that biomolecule conjugation reactions employing acylation with Bolton-Hunter type reagents, such as N-succinimidyl esters, are strongly influenced by solution pH and concentrations of the two reactants.[7–9] In order to obtain sufficient dose for microPET studies in an efficient and reproducible matter, performing small-scale experiments to explore several key reaction parameters to improve radiolabeling yield (RLY), as well as specific activity (SA) and immunoreactivity (IR) is necessary.[10] At bench scale, these efforts require large amounts of recombinant protein (on the order of milligrams) and repeated production of [^{18}F]SFB, discouraging the routine practice of such optimization procedures. In addition, the bench-scale approaches (even in the microliter scale) generally require manual operations which are labor-intensive and increase the risks of radiation exposure and operator error. An ideal solution would be to create a miniaturized reaction platform for screening a range of reaction conditions in order to identify optimal labeling parameters, with minimal consumption of biomolecules and radiolabeling agents.

Microfluidic devices, particularly based on the concept of using nanoliter droplets as microreactors, exhibit numerous advantages, including sample economy, precise control of reaction conditions, mixing, reproducibility and scalability for various chemical/biological applications.[11–17] Common methods of forming nanoliter droplets are creating emulsion by merging two immiscible fluids, such as water and oil. However, these implementations lack a practical means to generate composition-specific droplets on demand from scarce reagents and most of them utilize oil as carriers which might interfere with downstream chemical and biological experiments.[12, 17–21] Additional processes of oil removal and sample separation in a small volume can lead to significant loss of final product and elongate the total reaction time.

Hence reaction optimization using droplets (in oil) is often difficult to carry out in a reagent-economical fashion, a significant challenge when only small amounts of specialized biomolecules are available for labeling. On the other hand, using integrated microvalves, microfluidic batch reactors have demonstrated the digital automation and execution of complex on-chip chemical reactions and processes.[15, 22–24] Therefore, a promising approach

would be to confer digital control on a oil-free droplet generator by incorporating integrated microvalves into microchannel networks,[25] thus enabling sophisticated nanoliter-sized batch reactions and assays, which can be effectively harnessed for optimization of radiolabeling.

Herein, we demonstrate a new method to perform rapid screening and optimization of reaction parameters (pH and concentration) for labeling an anti-Prostate Stem Cell Antigen (PSCA) diabody (A2 Db) with [^{18}F]SFB. The entire process was carried out in a very sample-economic fashion by using a novel microvalve-based digital microfluidic droplet generation (DMDG) chip in an oil-free environment. The production of ^{18}F-labeled A2 Db (4-[^{18}F]fluorobenzolyated A2 Db, i.e. [^{18}F]FB-A2 Db) was successfully scaled up to produce sufficient quality and quantities of tracer for imaging mice with human prostate cancer xenografts.

Materials and Methods

Materials

Unless otherwise specified, all chemicals were of analytic grade and were commercially available. The preparations of ^{18}F-labeling agent, N-succinimidyl 4-[^{18}F]fluorobenzoate ([^{18}F]SFB), and A2 Db were illustrated in Supplemental Material. The prostate cancer xenograft LAPC-9, the B-cell lymphoma SKW6.4 and the PSCA-transduced SKW 6.4 cell lines were maintained as previously described.[26, 27]

Chip Structure and Operation

The microfluidic chip system was designed to provide a reliable miniaturized platform to generate composition-controlled droplets for screening labeling parameters using very small amount of reagents. A two-layer microvalve-based DMDG chip was designed, composed of three functional parts: (1) a droplet generation core, where specific quantities of reagents are measured and merged into composition-specific droplets; (2) a peristaltic pump, which produces serial compressed nitrogen pulses that can precisely deliver intact droplets to the desired location at constant speed and (3) a mixing channel for facilitating mixing process within each droplet (Fig. 1A and B). Inlets (from left to right) of droplet generation core are for cleaning solution 1, vacuum, cleaning solution 2 or buffer solution 1, [^{18}F]SFB, A2 Db, buffer solution, and pH control buffer 2, respectively, and port 8 is outlet for waste.

In a typical experiment, [^{18}F]SFB and A2 Db solutions are pipetted into small transfer vials (from 5 to 20 μL), which served as reservoirs to continuously supply reactants during optimizing the radiolabeling reactions. By actuating the microvalves using control channels with compressed air (*ca.* 414 kPa), a series of on-chip functions and operations can be executed. The droplets (*ca.* 120 nL/droplet) composed of three ratio-controlled components are produced one-by-one. The droplet generation process is digitally controlled by a PC within the droplet generation core and the sequences are as follows (see Supplemental Material for details): (1) vacuum is applied to remove residual gas inside each chamber; (2) the chamber is then filled with a different reagent (section **I, II**, and **III** in Fig. 1B); (3) the dividing microvalves are opened and their contents are merged to form a single multi-component droplet; (4) the droplets with specific compositions are driven into the mixing channel by compressed nitrogen. By changing reagents and/or adjusting the chamber volumes, droplets with pre-determined compositions can be generated. In general, it takes *ca* one minute to generate five droplets representing a given ^{18}F-labeling reaction condition. On-chip digital control to manipulate small volumes has enabled sophisticated nanoliter-sized batch reactions. In addition, the oil-free droplets can be directly collected, measured and used for the next step.

Adjustment of pH Condition (Figure 1D)

To adjust pH value of each ^{18}F-labeling reaction, different pH control buffers with a fixed volume [5 chamber units (*ca* 40 nL), **section III** in Fig. 1D] were introduced into each droplet along with the [^{18}F]SFB and A2 Db (v/v/v, 1:1:1) (Supplemental Material, Figure S6 and Table S3 for details). After cleaning droplet generation core and mixing channel, the pH value in each droplet can be easily adjusted by using a desired pH control buffer. 11 standard pH control buffers (pH 4.0, 4.5, 5.0, 5.5, 6.0, 8.0, 8.7, 10.0, 11.0, 12.0, 13.0) were applied for adjusting pH range in each ^{18}F-labeling reaction condition.

Adjustment of A2 Db Concentration (Figure 1E)

To adjust the concentration of A2 Db, **section II** in the droplet generator core was subdivided by microvalves into two individual chambers with different size ratios, which were then filled with A2 Db solution and dilution buffer (Fig. 1E), respectively. Using an A2 Db stock solution (2 mg/mL in optimized pH buffer), droplets with 7 different concentrations (from 0.13 to 1.3 mg/mL) were generated on-chip by combining **section II** and **III** (Supplemental Material).

Sample Collection and Radiochemistry Analysis

Sample droplets were stored and reacted within the sample outlet tube for 5 min and then directly dropped onto instant thin layer chromatography strips (iTLC, Biodex, Shirley, NY) for analysis. The final radiolabeling yields were determined by a gamma counter (Wizard 3, Perkin Elmer, Waltham, MA). In order to avoid cross-contamination between droplets of different pH, wash droplets (a combination of deionized (DI) water/pH 7.4 PBS buffer) were inserted between droplets for cleaning (Supplemental Material, Table S2).

Estimation of Effective Specific Activity (ESA)

Since the separation of [^{18}F]FB-A2 Db from A2 Db is practically difficult, the ratio of radioactivity of ^{18}F-labeled diabody over total mass of diabody used in radiolabeling reaction ([^{18}F]FB-A2 Db/A2 Db) is used to define “effective specific activity (ESA)“. To determine the radioactivity of [^{18}F]FB-A2 Db, radioactivity was measured by a dose calibrator (CRC-25R, Capintec, Ramsey, NJ). The concentration of A2 Db stock solutions was determined by UV absorption (at 280 nm). The molecular weight of A2 Db and its extinction coefficient were calculated based on its amino acid sequence (ProtParam Tool, ExPASy, SIB, Swissland). Calculated ESAs were derived by dividing radioactivity of [^{18}F]FB-A2 Db from the reaction mixture and total amount of diabody (in mmol, based on a molecular weight of 55,000 Da). The radioactivity of [^{18}F]FB-A2 Db was corrected by the radiochemical purity of crude reaction mixture determined by iTLC analysis.

Scale-up using Optimized Condition

Larger amount of [^{18}F]FB-A2 Db was produced at bench scale under the optimized condition. RLYs were measured by iTLC and size-exclusion HPLC (SEC-HPLC) [Biosep SEC S-2000 (Phenomenex, Torrance, CA)]. Radiolabeled diabody was purified by a spin column [Micro Biospin 6 column (Bio-Rad, Hercules, CA)]. The radiochemical purity of [^{18}F]FB-A2 Db was determined by iTLC and SEC-HPLC [PBS buffer (pH 7.4), flow rate: 1 mL/min, UV 254 and 280 nm, t_R= 5.1 min].

Immunoreactivity Assay

The immunoreactive fraction of [^{18}F]FB-A2 Db was determined by incubating its SEC-HPLC purified fraction [0.1 μCi (*ca* 0.01μg)] with large excess (*ca* 2×10^7 cells) of, either SKW6.4-PSCA (PSCA over-expressing), SKW6.4 cells (negative control) or no cells in 1 mL (PBS, 1% FBS) for 40 minutes at room temperature After incubation, cells were spun

down (800 × g) and 0.7 mL of supernatant was counted in a gamma counter. Experiments were carried out in duplicate. The immunoreactivity was determined as the fraction that bound to the cells (SKW6.4-PSCA) compared to the control (no cells).

MicroPET/CT Imaging and Biodistribution Studies

All animal studies were conducted under protocols approved by the Chancellor's Animal Research Committee at the University of California, Los Angeles. LAPC-9 xenografts were established in 7- to 8-week-old male SCID mice (Charles River Laboratories, Wilmington, MA) by s.c. inoculation of LAPC-9 cells (*ca* 10^6 cells) near the shoulder. After 14 to 21 days, when tumor masses were in the range of 100–300 mg, [^{18}F]FB-A2 Db (50–99 μCi) was injected into the tail vein of each animal. Mice were serially imaged using a microPET (Focus 220 scanner, Siemens Preclinical Solutions, Knoxville, TN). To enable imaging, mice were anesthetized using 2% isoflurane, positioned in a prone position along the long axis of the microPET scanner and imaged. Images were reconstructed using a filtered back projection reconstruction algorithm. Directly after the microPET scan, a computed tomography (CT) scan was performed using a microCT (microCAT II, Concorde Microsystems, Knoxville, TN) for 10 min. After the final CT scan, mice were euthanized and tumors, liver, spleen, kidney, lung, and blood were harvested, weighed and counted in a gamma counter. Results were calculated as percentage of injected dose per gram (% ID/g) of tissue. For image analysis, cylindrical regions of interest (ROI) were drawn from three-dimensional filtered back projection (FBP) reconstructed PET/CT co-registered images using AMIDE as previously described. Four ROIs were drawn within the tumor and another four in the arm muscle region in the low activity areas close to the tumors and termed ‘background’.

Results

Optimization of pH and Concentration on Chip

Using our DMDG chip, we rapidly screened 11 radiolabeling conditions with different pHs, ranging from 5 to 10. At a constant A2 Db concentration [stock solution: 2 mg/mL; droplet: 0.66 mg/mL in PBS buffer (pH 7.4)], the maximum RLY was obtained at pH 8.7 (Supplemental Material, Fig. S7). In order to confirm these findings, the pH of A2 Db stock solution was readjusted to 8.7, the screening experiments were repeated, and results again showed that the optimal pH was indeed 8.7 (n=5; Fig. 2A). Separately we also confirmed that A2 Db was stable over a pH range of 7.5–10 and showed very little loss in binding activity (Supplemental Material, Fig. S2b). Using our DMDG chip, the concentration of A2 Db in each droplet ranged from 0.13 to 1.33 mg/mL were generated by changing the volume ratios between A2 Db and pH 8.7 buffer in both **section II** and **III** in the droplet generation core (Supplemental Material, Fig. S8). As shown in **Figure 2B**, the RLY of diabody with [^{18}F]SFB was strongly concentration-dependent. The RLY was *ca* 8% at the A2 Db concentration of 0.25 mg/mL and increased to 27% at 1 mg/mL.

Determination of Optimal Conditions

The calculated ESAs were determined based on the final radioactivity of [^{18}F]FB-A2 Db according to RLYs in each microfluidic-based experiment and the amount of Db in each droplet. Although RLYs of diabody labeling reactions increased as concentration of Db increased (Fig. 2B), the ESAs actually declined at Db concentrations above 0.5 mg/mL. Therefore, in order to maintain reasonably high labeling yield to provide sufficient amount of [^{18}F]FB-A2 Db for microPET studies while obtaining tracers with highest SA, we selected 0.66 mg/mL (pH 8.7) as the optimal concentration for scale-up.

Scale-up from Microfluidics to Bench Scale

Prior to scale-up, it is critical to determine whether the optimal labeling conditions obtained on-chip could be directly translated into a bench-scale run. To do so, we repeated the pH optimization study off-chip using a bench-scale reaction. [^{18}F]SFB [25 μL in PBS buffer (pH 7.4)] and A2 Db [50μL (1 mg/mL) in buffers with various pHs] were mixed and incubated in vials at 30°C for 5 minutes. In these bench-scale experiments, maximal RLY (25.8%) was also observed at pH 8.7 (Fig. 2C), demonstrating good agreement between optimal conditions found by bench-scale and on-chip approaches. Small batches of [^{18}F]FB-A2 Db from on-chip and bench-scale labeling were produced under the optimized labeling conditions [A2 Db concentration: 0.66 mg/mL in sodium borate buffer (pH 8.7); for 5 min at 30°C]. Size-exclusion chromatographic analyses of those two crude reaction mixtures showed high similarity (Supplemental Material, Fig. S9). Following a simple spin-column purification, sodium dodecyl sulfate-polyacrylamide gel electrophoresis (SDS-PAGE) and autoradiographic imaging (Fig. 2D) analyses also confirmed the formation of [^{18}F]FB-A2 Db with high radiochemical purity in both approaches. The radiochemical purity of [^{18}F]FB-A2 Db was also determined by SEC-HPLC (>95%) (Supplemental Material, Fig. S10). Under the optimized condition, about 6–10 mCi of [^{18}F]FB-A2 Db was produced from 20–35 mCi of [^{18}F]SFB in 10–20 min.

Immunoreactivity

It is of critical importance that proteins, such as diabodies, still retain their biological function after ^{18}F-labeling. Using PSCA-over-expressing SKW 6.4-PSCA cells and parental SKW 6.4 cells (negative control), the immunoreactivity of purified [^{18}F]FB-A2 Dbs prepared from both approaches (microfluidic and bench-scale) were determined. After 40 minutes incubation with cells at ambient temperature, both [^{18}F]FB-A2 Dbs showed similar high immunoreactivities (*ca* 68±1% (s.d.), Fig. 3A).

MicroPET/CT Imaging and Biodistribution Studies

The calculated ESAs of the final [^{18}F]FB-A2 Dbs ranged from 14.8–20.4 TBq/mmol (400–550 Ci/mmol) after a simple spin-column purification, and radiochemical purities were >95% (Supplemental Material, Fig. S10). In a typical microPET study, [^{18}F]FB-A2 Db (85–100 μCi) was injected intravenously into tumor-bearing mice (n=3), and a dynamic scan was performed from 0 to 110 min (Fig. 3B). Tumor locations were visualized on microPET/CT images *ca* 20–30 min p.i. due to a combination of increase tumor signal and rapid blood clearance. As expected, the majority of the [^{18}F]FB-A2 Db cleared through the kidneys; a portion of the radioactivity cleared via gallbladder and intestines, which was also observed for hydrolyzed [^{18}F]SFB (i.e. 4-[^{18}F]fluorobenzoic acid) (Supplemental Material, Fig. S11). At 4 h p.i., microPET images showed high tumor contrast and clear imaging were obtained (Fig. 3B) with a target-to-background ratio of 13.6±2.5 determined by ROI analysis of LAPC-9 tumor versus soft tissue. This is consistent with the biodistribution data (4 h p.i.) which demonstrated that most of the activity had cleared from major organs resulting in a higher tumor uptake [3.13 % injected dose per gram (ID/g)] compared to liver, spleen, kidneys, and lungs uptakes (Fig. 3C). The tumor-to-blood ratio for the LAPC-9 tumors using [^{18}F]FB-A2 Db was 4.8 at 4 h.

Discussion

Imaging of cell surface biomarkers is emerging as an increasingly important approach in cancer detection and monitoring therapeutic efficacy. We have previously shown that engineered antibody fragments (i.e. diabodies and minibodies) retain excellent tumor targeting in mouse models *in vivo*, coupled with rapid clearance from the circulation. Since the pharmacokinetic of diabodies match very well with the half-life of F-18,[6] their ^{18}F-

labeled versions represent a novel class of PET tracers with broad potential utility for imaging cell surface phenotype *in vivo*. Therefore there is a great need for developing efficient procedures to produce ^{18}F-labeled diabody-based tracers in high yield sufficient for routine PET imaging.

Because the amounts of proteins produced in the R&D environment are often restrained, the extent to which trial-and-error optimizations of the [^{18}F]SFB labeling reactions can be conducted is rather limited. Alternatively, brute force approaches using entire batches of proteins and high activity (>1 Ci) were often used to ensure sufficient activity produced for microPET studies.[6] Therefore, a practical means to perform optimization using only small amount of proteins and radiolabeling tags is critical to the progress of this field. Since the minute masses required for radiotracer production are well matched to the small volumes required in microfluidics, we have designed and fabricated a DMDG chip which can "digitally" generate composition-specific and size-controlled droplets on demand. This microfluidic-based optimization method provides a simple and effective means to perform screening pH and concentration droplet-by-droplet. The unique features of this device allow: (1) the independent control of volume and composition for every droplet, enabling reaction condition screening with minimal reagent consumption (Supplemental Material, Movie S1); (2) the ability to pause, modify, and restart the droplet generation process, e.g. for replacement/change of reagents (Supplemental Material, Movie S2); and (3) the use of nitrogen gas rather than oil to separate droplets, eliminating the need for oil removal steps later. Furthermore, the current device, distinct from other droplet-based microfluidics,[14, 28] is unique in its ability to operate with very low total volumes of samples and reagents with little to no loss. As each droplet can be driven out slowly in a well-controlled matter using the on-chip peristaltic pump, one single droplet can be easily used for determining the corresponding RLY. The volume and radioactivity of a single droplet is around 120 nL and can represent 0.5–2 μCi, respectively. For example, 5 μL of diabody solution (2 mg/mL) could be used in screening for more than 125 different conditions in single micro-droplets.

To probe specific biological process *in vivo* without exerting mass effects within the same living systems under study, for example, measuring receptor-ligand interactions, PET tracers with high SA are desired. Our strategy to obtain ^{18}F-labeled diabody of high SA (in our case, ESA) is to first, identify the pH range leading to the highest RLY, and subsequently optimize the protein concentration to generate the highest ESA at the previously-determined optimal pH. In the [^{18}F]SFB labeling reactions, RLYs generally increase at higher protein concentrations at the optimal pH. However, continuing to increase the amount of protein used in the labeling reaction will lower the final ESA since the RLY eventually plateaus (Fig. 2B). Using our DMDG chip, a series of experiments with different pHs and concentrations can be rapidly performed, allowing mapping the area of optimal conditions. This is especially important since the optimal parameters for [^{18}F]SFB labeling vary depending on the sequence and structure of the individual protein being radiolabeled. Furthermore, batch-to-batch variations can occur for the protein and [^{18}F]SFB as well, making rapid optimization using small aliquots of reactants even more critical. Our method utilizing the DMDG chip can address requirements above by identification of optimal reaction parameters in a rapid, reagent-economical fashion. Once the optimal reaction parameters are identified, larger-scale reactions can be performed under the same chip-derived conditions to produce sufficient amount of ^{18}F-labeled biomolecules.

Compared to the previously described ^{124}I-labeled minibody currently in clinical development,[29] the new [^{18}F]FB-A2 Db opens the possibility of same-day PET imaging with superior image contrast in a clinical setting. The key advantage of using diabodies, the smallest bivalent fragments based on antibody combining sites, is the potential to obtain clear tumor visualization just a few hours (4–6 h) after injection [30]. Earlier microPET

imaging results using ^{124}I-labeled anti-PSCA diabodies suggested that the best image contrast required a 12 h delay and the tumor-to-blood (ROI) ratio was around 3[31]. In contrast, the tumor-to-soft tissue ratio using [^{18}F]FB-A2 Db in this study was 13.6 at 4 h p.i., which represents a significant improvement. There are several possible explanations for this improvement. First, the half-life and positron yield of F-18 is better suited for PET detection within 4–6 h p.i. Second, due to the optimization of microfludic method, the resulting [^{18}F]FB-A2 Db was obtained with high immunoreactivity to PSCA, radiochemical purity and ESA. Third, the radioiodination method used to label anti-PSCA diabodies [27] was not optimal and could result in deiodination that can affect the tumor uptake and reduce image contrast. It is difficult to isolate the degree of influence among those individual parameters from *in vivo* imaging results, and it is likely that all of the factors listed above are important. Regardless, in order to obtain an effective protein-based immunoPET tracer, it is necessary to optimize individual ^{18}F-labeling condition under which a sufficient amount of tracer with high immunoreactivity, ESA and radiochemical purity can be generated.

To show the versatility and generality of our method, we also applied this microfluidic-based method to optimize the [^{18}F]SFB labeling of an additional diabody (anti-HER2 Db) specific to Human Epidermal Growth Factor Receptor 2 (HER2) and, under optimized conditions (Supplemental Material, Fig. S12), [^{18}F]FB-anti-HER2 Db was obtained for microPET studies in a breast cancer xenograft-bearing mouse (MCF-7/HER2) (Supplemental Material, Fig. S13). These successful examples utilizing a microfluidic-based approach for optimization of labeling conditions provide a practical means to produce [^{18}F]fluorobenzoylated diabodies ([^{18}F]FB-labeled Dbs) or other scarce biomolecules. Furthermore, our microfluidic-based method is a *de novo* approach and can be applied in the beginning of each labeling experiment to access the quality of biomolecule and determine of best labeling condition for the day.

Conclusion

A rapid and efficient method was developed to ^{18}F-label diabodies by scouting conditions using a DMDG chip. Reaction parameters (pH and diabody concentration) were analyzed in individual droplets, requiring only very small amounts of protein (diabody) and [^{18}F]SFB. 200- to 2000-fold reduction in protein consumption can be achieved, compared to conventional bench-scale approaches, during the optimization stage. Optimal labeling conditions identified by a DMDG chip was then translated into efficient scale-up of [^{18}F]FB-A2 Db suitable for *in vivo* evaluation. This versatile microfluidic-based method has potential to be employed efficiently for radiolabeling of a diverse spectrum of biomolecules, including intact antibodies and their fragments, other proteins, and peptides, etc., which can ultimately accelerate investigations using novel biological PET tracers.

Supplementary Material

Refer to Web version on PubMed Central for supplementary material.

Acknowledgments

This work was supported by funding from US Department of Energy (DE-PS02-09ER09-08 and DE-PS02-09ER09-18), National Institute of Health (CA 092131 and CA 086306), UC Discovery Grant (bio07-10665) and UCLA Jonsson Comprehensive Cancer Center (CA016042). We thank N. Satyamurthy and his staffs for providing F-18 ion and many useful discussions, H.-D. Lin, C. Xia, and D.A. Williams for assisting with radiolabeling chip and system design, R. Reiter and colleagues for providing the mouse models, and T. Olafsen, D. Stout, W. Ladno and J. Edwards for assistance with the microPET studies.

References

1. Phelps ME. Positron emission tomography provides molecular imaging of biological processes. Proc Natl Acad Sci U S A. 2000; 97:9226–9233. [PubMed: 10922074]
2. Czernin J, Phelps ME. Positron emission tomography scanning: Current and future applications. Annu Rev Med. 2002; 53:89–112. [PubMed: 11818465]
3. Weber WA. Positron emission tomography as an imaging biomarker. J Clin Oncol. 2006; 24:3282–3292. [PubMed: 16829652]
4. Vaidyanathan G, Zalutsky MR. Labeling proteins with F-18 using N-succinimidyl 4-[F-18]fluorobenzoate. Nucl Med Biol. 1992; 19:275–281.
5. Okarvi SM. Recent progress in fluorine-18 labelled peptide radiopharmaceuticals. Eur J Nucl Med. 2001; 28:929–938. [PubMed: 11504093]
6. Cai WB, Olafsen T, Zhang XZ, et al. PET imaging of colorectal cancer in xenograft-bearing mice by use of an F-18-labeled T84.66 anti-carcinoembryonic antigen diabody. J Nucl Med. 2007; 48:304–310. [PubMed: 17268029]
7. Li JL, Trent JO, Bates PJ, Ng CK. Factors affecting the labeling yield of F-18-labeled AS1411. J Labelled Compd Rad. 2007; 50:1255–1259.
8. Zijlstra S, Gunawan J, Burchert W. Synthesis and evaluation of a F-18-labelled recombinant annexin-V derivative for identification and quantification of apoptotic cells with PET. Appl Radiat Isotopes. 2003; 58:201–207.
9. Garg PK, Garg S, Zalutsky MR. F-18 labeling of monoclonal-antibodies and fragments with preservation of immunoreactivity. Bioconjugate Chem. 1991; 2:44–49.
10. Vaidyanathan G, Zalutsky MR. Protein radiohalogenation: Observations on the design of N-succinimidyl ester acylation agents. Bioconjugate Chem. 1990; 1:269–273.
11. Talu E, Hettiarachchi K, Zhao S, et al. Tailoring the size distribution of ultrasound contrast agents: Possible method for improving sensitivity in molecular imaging. Mol Imaging. 2007; 6:384–392. [PubMed: 18053409]
12. Liu K, Ding HJ, Liu J, et al. Shape-controlled production of biodegradable calcium alginate gel microparticles using a novel microfluidic device. Langmuir. 2006; 22:9453–9457. [PubMed: 17042568]
13. Thorsen T, Maerkl SJ, Quake SR. Microfluidic large-scale integration. Science. 2002; 298:580–584. [PubMed: 12351675]
14. Song H, Chen DL, Ismagilov RF. Reactions in droplets in microflulidic channels. Angew Chem Int Edit. 2006; 45:7336–7356.
15. Lee CC, Sui GD, Elizarov A, et al. Multistep synthesis of a radiolabeled imaging probe using integrated microfluidics. Science. 2005; 310:1793–1796. [PubMed: 16357255]
16. Mark D, Haeberle S, Roth G, et al. Microfluidic lab-on-a-chip platforms: requirements, characteristics and applications. Chem Soc Rev. 2010; 39:1153–1182. [PubMed: 20179830]
17. Liu K, Ding HJ, Chen Y, Zhao XZ. Droplet-based synthetic method using microflow focusing and droplet fusion. Microfluid Nanofluid. 2007; 3:239–243.
18. Hong JW, Quake SR. Integrated nanoliter systems. Nat Biotechnol. 2003; 21:1179–1183. [PubMed: 14520403]
19. Pregibon DC, Toner M, Doyle PS. Multifunctional encoded particles for high-throughput biomolecule analysis. Science. 2007; 315:1393–1396. [PubMed: 17347435]
20. Beer NR, Hindson BJ, Wheeler EK, et al. On-chip, real-time, single-copy polymerase chain reaction in picoliter droplets. Anal Chem. 2007; 79:8471–8475. [PubMed: 17929880]
21. Abdelgawad M, Watson MWL, Wheeler AR. Hybrid microfluidics: A digital-to-channel interface for in-line sample processing and chemical separations. Lab Chip. 2009; 9:1046–1051. [PubMed: 19350085]
22. Wang JY, Sui GD, Mocharla VP, et al. Integrated microfluidics for parallel screening of an in situ click chemistry library. Angew Chem Int Edit. 2006; 45:5276–5281.
23. Gerber D, Maerkl SJ, Quake SR. An in vitro microfluidic approach to generating protein-interaction networks. Nat Methods. 2009; 6:71–74. [PubMed: 19098921]

24. Chung KH, Crane MM, Lu H. Automated on-chip rapid microscopy, phenotyping and sorting of C. elegans. Nat Methods. 2008; 5:637–643. [PubMed: 18568029]
25. Liu K, Chen Y, Tseng H, et al. Microfluidic device for robust generation of two-component liquid-in-air slugs with individually controlled composition. Microfluid Nanofluid. 2010 Accepted.
26. Craft N, Chhor C, Tran C, et al. Evidence for clonal outgrowth of androgen-independent prostate cancer cells from androgen-dependent tumors through a two-step process. Cancer Res. 1999; 59:5030–5036. [PubMed: 10519419]
27. Leyton JV, Olafsen T, Lepin EJ, et al. Humanized radioiodinated minibody for imaging of prostate stem cell antigen-expressing tumors. Clin Cancer Res. 2008; 14:7488–7496. [PubMed: 19010866]
28. Teh SY, Lin R, Hung LH, Lee AP. Droplet microfluidics. Lab Chip. 2008; 8:198–220. [PubMed: 18231657]
29. Gagnon P, Cheung CW, Lepin EJ, et al. Minibodies and multimodal chromatography methods. BioProcess International. 2010; 8:26–35.
30. Wu AM, Yazaki PJ. Designer genes: recombinant antibody fragments for biological imaging. Q J Nucl Med. 2000; 44:268–283. [PubMed: 11105590]
31. Leyton JV, Olafsen T, Sherman MA, et al. Engineered humanized diabodies for microPET imaging of prostate stem cell antigen-expressing tumors. Protein Eng Des Sel. 2009; 22:209–216. [PubMed: 18957406]

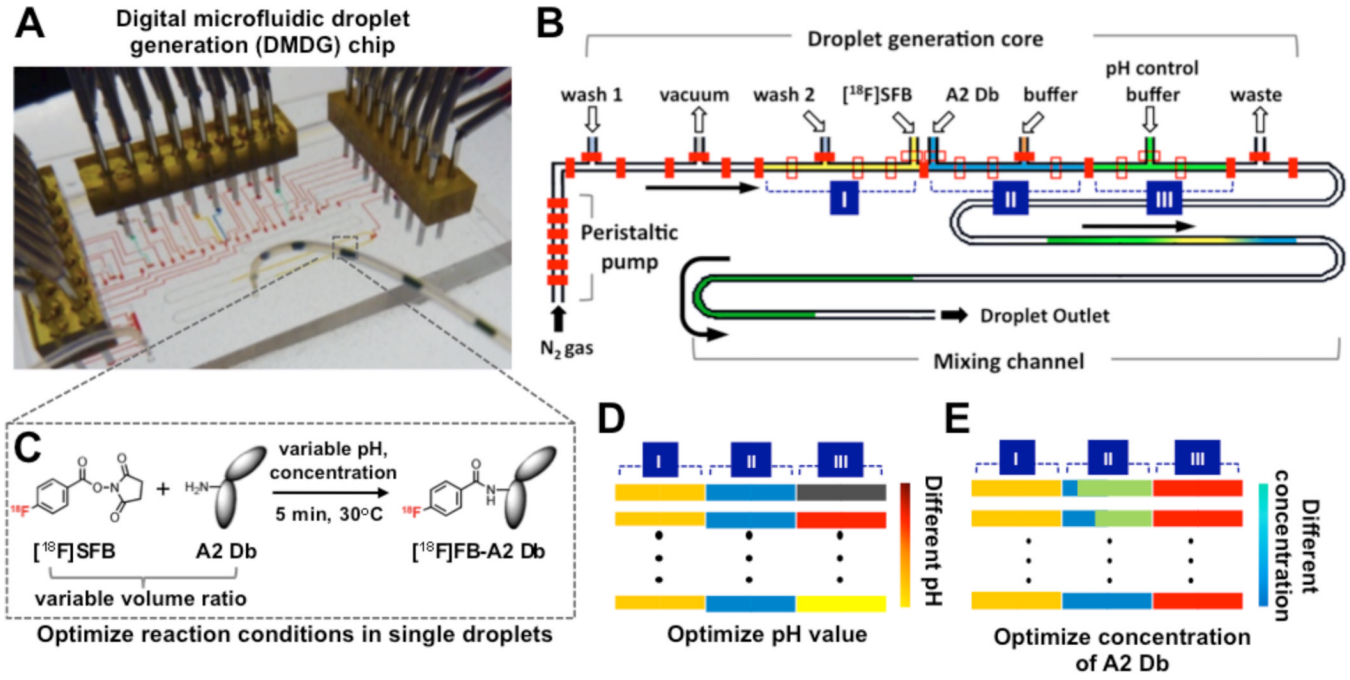

Figure 1.

Schematic illustrations of the detailed architecture of a digital microfluidic droplet generation (DMDG) chip, working principle and chip-based screening. (**A**) A setup of DMDG chip in which food dyes were used to aid visualization of different components; (**B**) Schematic of a DMDG chip. The DMDG chip is composed of three functional parts: (1) droplet generation core, where droplets with specific compositions can be generated digitally; (2) on-chip peristaltic pump, which precisely produces serial compressed nitrogen pulses that can reliably deliver intact droplets to the desired location and (3) mixing channel. Inlets 1–8 are for cleaning, vacuum, cleaning/buffer 1, [^{18}F]SFB, A2 Db, buffer 2, pH control buffer, and waste respectively. Section I is specifically used for [^{18}F]SFB, section II for A2 Db and buffer 2, section III for pH control buffer, respectively. The fluidic channel width is *ca* 200 μm and height is *ca* 40 μm. (**C**) The reaction scheme of ^{18}F-labeling diabody using [^{18}F]SFB. (**D**) Schematic of adjusting pH in each droplet. (E) Schematic of adjusting the concentration of A2 Db in each droplet.

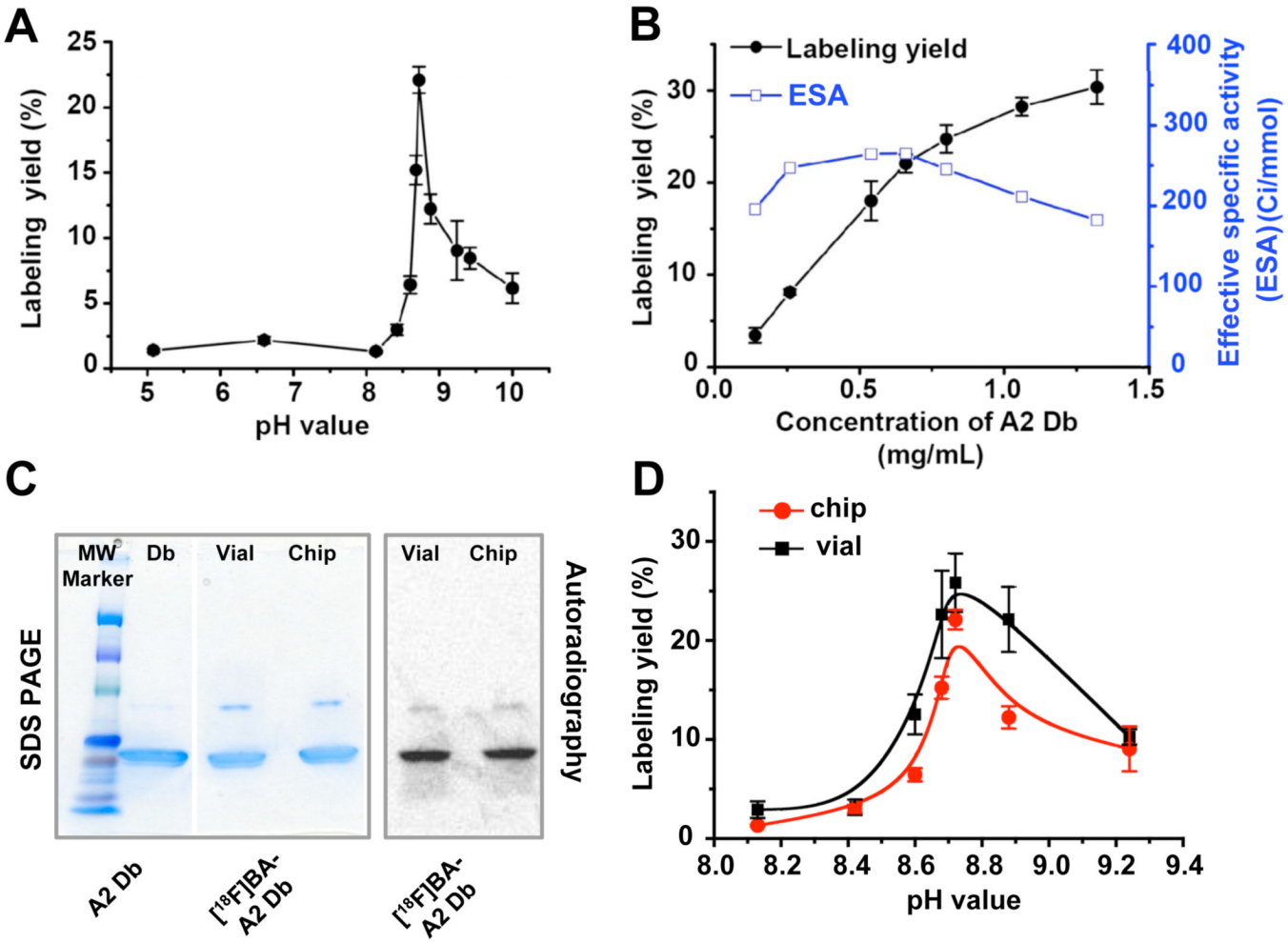

Figure 2.

(**A**) The effect of pH on RLY (n=3). (**B**) The effect of diabody concentration on RLY at pH 8.7 (n=3). (**C**) Unlabeled A2 Db, and [^{18}F]FB-A2 Db produced from bench-scale vial and microfluidic chip were run on SDS-PAGE and analyzed by autoradiography. Proteins were later revealed by Coomasie blue staining. (**D**) Compare RLY by using conventional bench-scale method and on-chip approach (n=3).

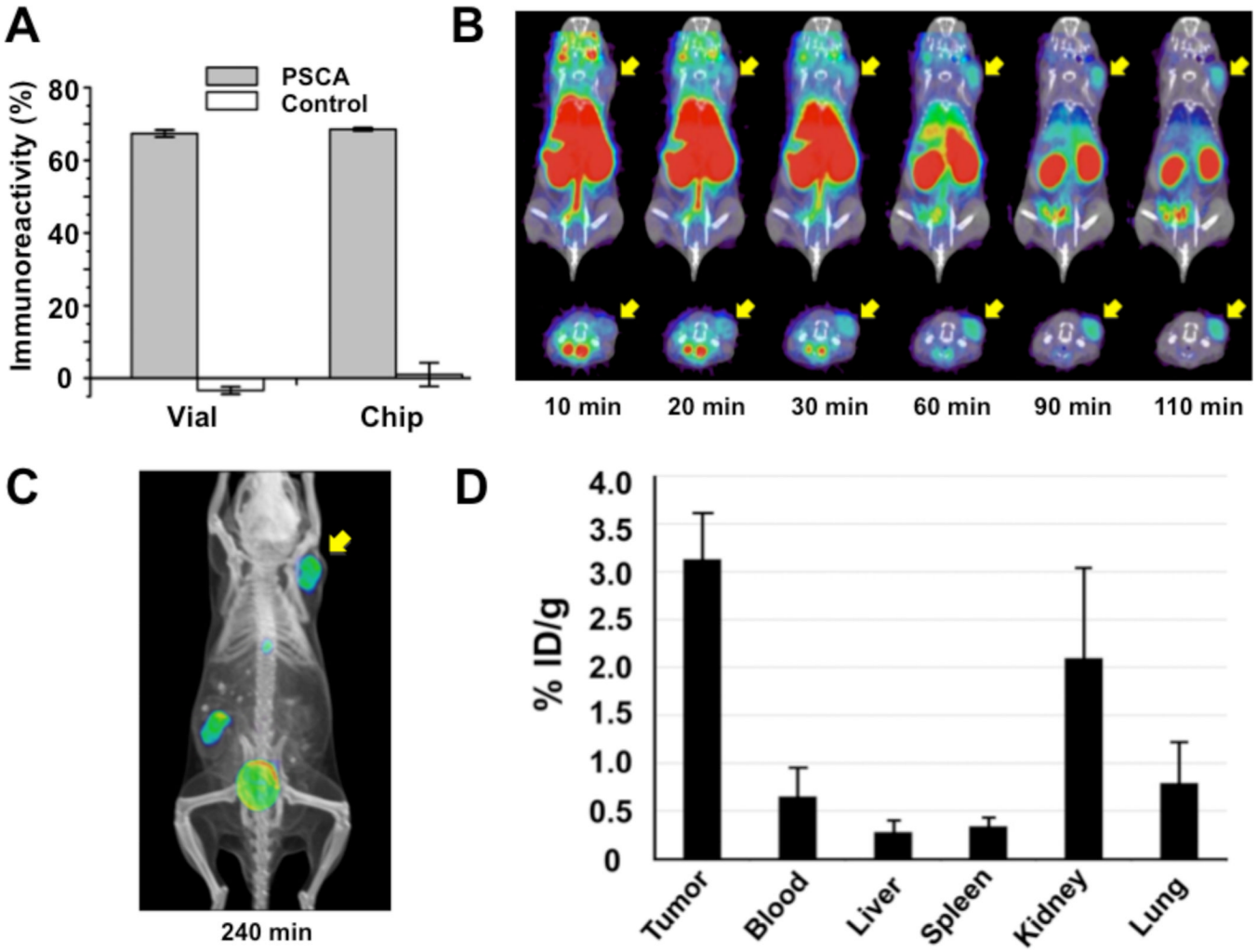

Figure 3.

Biochemical, *in vitro* and *in vivo* characterizations of [^{18}F]FB-A2 Db. (**A**) Immunoreactivity of [^{18}F]FB-A2 Db produced from vial or chip to PSCA-expressing SKW 6.4 and SKW 6.4 cells (control) (n=2). (**B**) Co-registered microPET/CT dynamic scan images (coronal [top] and transverse [bottom] slices) of nude mice bearing LAPC-9 (PSCA-positive human prostate cancer) xenografts. Tumor locations are indicated by yellow arrows. (**C**) A co-registered microPET/CT image (coronal projections) 4h p.i. of [^{18}F]FB-A2 Db. (**D**) Graph of biodistribution study of [^{18}F]FB-A2 Db (4 h p.i.) (n=3).